

# Enhancement in photoluminescence emission in the UV-visible region from chemically synthesized silver doped ZnS nanoparticles

R. Sarkar, P. Kumbhakar and A.K. Mitra

Nanoscience Laboratory, Department of Physics, National Institute of Technology,  
Durgapur, 713209, India

\*Corresponding author, Tel : +91-343-2546808, Fax:+91-343-2547375

\*E-mail: [nitdgpkumbhakar@yahoo.com](mailto:nitdgpkumbhakar@yahoo.com) & [pathik.kumbhakar@phy.nitdgp.ac.in](mailto:pathik.kumbhakar@phy.nitdgp.ac.in)

## ABSTRACT

Nanoparticles of ZnS:Ag doped with Ag<sup>+</sup> (0.5%) and capped with polyvinyl pyrrolidone (PVP) have been synthesized by chemical co-precipitation method. The particle size of the synthesized sample is ~2.5 nm as obtained from the analyses of X-ray diffraction (XRD) pattern and high resolution transmission electron microscope (HRTEM) image of the sample. The optical absorption and photoluminescence (PL) emission properties are measured by using UV-visible spectrophotometer and PL spectrometer, respectively. The quantum confinement effect is demonstrated by the blue shift in the bandgap of the sample. The Gaussian fittings of the measured room-temperature PL spectrum shows the presence of six emission bands centered at 356.5, 393, 449, 483, 508, and 526 nm. However, the intensity of the emission band at 394 nm in ZnS:Ag sample is the strongest and it is ~60 times more intense than that of the PL emission intensity obtained in an undoped ZnS sample.

**Keywords:** Nanostructures; Semiconductors; Chemical synthesis; Optical properties

## 1. INTRODUCTION

Doped II-VI semiconductors ZnS nanoparticles (NPs) are of great current interest due to their unique electronic and optical properties and for their potential technological application as a phosphor for photoluminescence (PL), electroluminescence (EL) and cathodoluminescence (CL) devices [1-10]. ZnS and doped ZnS NPs are also suitable for applications in high-capacity communication networks, optoelectronics, biophotonic devices and especially for fluorescence imaging in living tissues due to their high refractive indices, multiphoton absorption properties and wide band gap characteristics [11, 12]. The tuning and enhancement in PL emissions in the visible region in ZnS NPs by Mn and Co doping and also by thermal annealing of undoped ZnS NPs have also been reported by us previously [2,13-14]. Luminescence studies of ZnS doped with impurities have sparked intensive interest as the impurity states in a doped ZnS can play a special role in affecting the electronic energy structures and PL emission characteristics. Few attempts have been made in the past for

improving the luminescence of ZnS/Mn, Ag thin film for electroluminescent devices and reported intense fluorescence emissions in the visible region [15-20]. However, here we report the synthesis of polyvinyl pyrrolidone (PVP) capped ZnS:Ag NPs of ~2.5 nm in sizes by the industry viable chemical precipitation method. The synthesized NPs exhibit wide and ~ 60 times enhanced PL emission covering the visible region in comparison to that of an undoped sample. From the Gaussian fitting of the PL spectrum it is found that it consists of six emission peaks at 356.5, 393, 449, 483, 508, and 526 nm. The strongest PL peak appeared at 393 nm (~3.15 eV) in ZnS:Ag NPs is attributed to the recombination of an excited electron either from the conduction band or some shallow traps just below the bottom of the conduction band with a positive hole captured at the acceptor level of silver. Photoluminescence emission appeared in the blue region peaked at 449 nm is attributed to defect-related emission of the ZnS host and the green peak appeared at 525 nm is due to a transition either from an impurity donor level or lattice defects at 0.91 eV below the lower edge of the conduction band to silver acceptor level. The presented results would be valuable to develop highly efficient luminescent devices based on metal ion doped semiconductor nanomaterials.

## 2. EXPERIMENTAL

### 2.1 Materials

Poly vinyl pyrrolidone (PVP), zinc nitrate, zinc sulphide, silver nitrate and all other chemicals (AR grade) used are purchased from Mark & SD fine chemical and they are used as-received without further treatment.

### 2.2. Synthesis of the nanomaterials

The synthesis of the nanomaterials is carried out at room temperature by chemical co-precipitation method. At first 20ml solution of both zinc nitrate and sodium sulphide in methanol and 10 ml solution of silver nitrate in methanol are prepared. Zinc nitrate solution is vigorously stirred with the addition of silver nitrate solution and 0.3mM PVP solution using a magnetic stirrer upto 1hr, then solution of sodium sulphide and manganese salt are mixed drop wise upto pH-8.

The white precipitate is separated from the reaction mixture by centrifugation for 5min at 10,000 rpm and washed several times with methanol to remove all sodium particles. The sample is then dried and collected a part of it for characterization of nanostructural and optical and properties.

### 2.3. Characterization

X-ray diffraction (XRD) pattern of the sample has been recorded using an X-ray diffractometer (PANALYTICAL) using Cu  $K_{\alpha}$  radiation of wavelength  $\lambda = 0.15406$  nm in the scan range of  $2\theta = 20-80^{\circ}$ . For collecting the XRD pattern powder samples of NPs are kept on the sample holder. The particle size distribution of the as-synthesized ZnS:Ag NPs was confirmed using high resolution transmission electron microscope (HRTEM, JEOL, JEM-2100). The optical absorption spectra of the sample are recorded using a UV-VIS spectrophotometer (Hitachi, U-3010). Photoluminescence (PL) spectra of all the samples are recorded at room temperature and measured by a spectrofluorimeter (LS55, Perkin Elmer). For the PL measurement also NPs are dispersed in methanol and kept in a standard four sides polished cuvette of 10mm path length.

## 3. RESULTS AND DISCUSSIONS

X-ray diffraction pattern of the prepared ZnS:Ag NPs is shown in Fig.1. From the Fig. 1, it is further observed that four XRD peaks, appeared at the positions ( $2\theta$ ) 28.9, 47.9, 56.7, and 70.5 due to reflections from (111), (220), (311), and (400) planes of cubic ZnS (JCPDF 80-0020), respectively. In addition, another four appeared at 29.7, 38.8, 55.6, and 63.6 are due to reflections from (101), (110), (200), and (202) planes of Hexagonal ZnS (JCPDF 75-1534), respectively. The average crystalline size is  $\sim 2.5$  nm as calculated by using the Debye Scherer formula [2] and from full width at half maxima (FWHM) of the most intense XRD peak for the cubic phase. The Debye Scherer formula is given as,

$$D = 0.89\lambda / \beta \cos \theta \quad (1)$$

Where,  $D$  is the mean grain size,  $\lambda$  is X-ray wavelength,  $\beta$  is FWHM of diffraction peaks and  $\theta$  is diffraction angle. It is necessary to obtain the particle size and information about nanostructure by direct measurement, such as HRTEM which can reveals the size and morphology of the particles. Figures 2 shows the typical HRTEM image of the sample and inset of Fig. 2b shows its corresponding particle size-distribution. The average size of particles is  $2.54 \pm 0.04$  nm as obtained from the log-normal fitting of the measured particle-size distribution. The exciton Bohr diameter of ZnS is 4.4 nm, so the size of the synthesized ZnS:Ag NPs lie in the quantum confinement region. The inset of Fig. 2(a) shows the corresponding selected area diffraction (SAED) pattern, which confirmed the presence of cubic phase in the sample. The interplanner spacing ( $d_{hkl}$ ) as calculated from

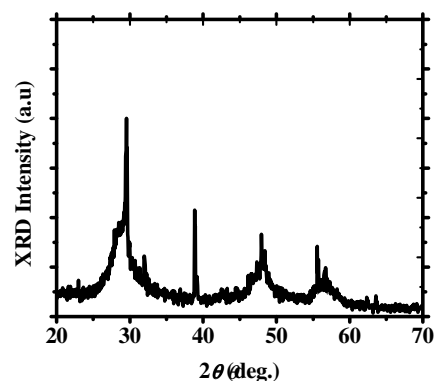


Figure 1: X-ray diffraction (XRD) pattern of the prepared ZnS:Ag sample.

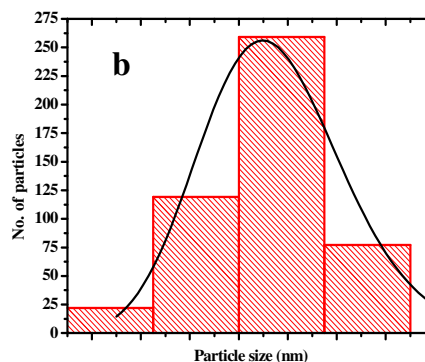
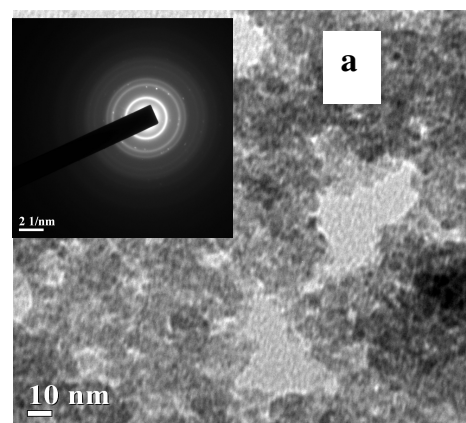


Figure 2: HRTEM micrograph of ZnS:Ag nanoparticles. Inset shows (a) selected area diffraction pattern (SAED) of sample and (b) corresponding particle size distribution of the sample.

(hkl)	$d_{JCPDS}$ (Å)	$d_{XRD}$ (Å)	$d_{HRTEM}$ (Å)
(111)	3.123	3.115	3.067
(220)	1.912	1.904	1.739
(311)	1.633	1.632	1.435

Table 1: Calculation of the inter-planar spacing corresponding to the cubic phase of ZnS:Ag sample.

SAED pattern, XRD and JCPDS data and corresponding (h k l) values are summarized in the Table 1.

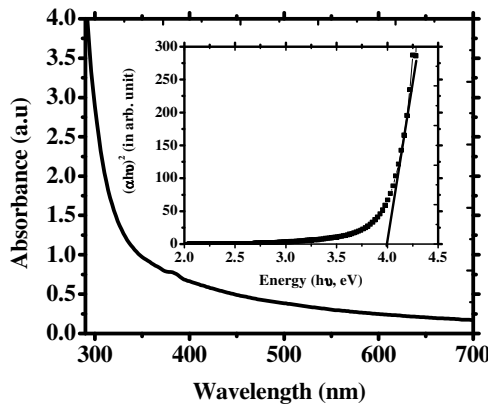


Figure 3: UV-visible absorption characteristics of ZnS:Ag sample. Inset shows the band gap calculation.

The linear optical absorption characteristics of the sample are also measured and it is shown in Fig. 3. For obtaining the absorption characteristics of the sample, at first the transmittance ( $T$ ) at different wavelengths ( $\lambda$ ) are measured and then absorption coefficient ( $\alpha$ ) at the corresponding wavelength  $\lambda$  is calculated using the Beer-Lambert's relation.

$$\alpha = \frac{1}{d} \ln\left(\frac{1}{T}\right), \quad (2)$$

where,  $d$  is the path length. The relation between the incident photon energy ( $h\nu$ ) and the absorption coefficients ( $\alpha$ ) is given by the following relation.

$$(\alpha h\nu)^{1/m} = c(h\nu - E_g), \quad (3)$$

where,  $c$  is a constant and  $E_g$  is the bandgap of the material and the exponent  $m$  depends on the type of the transition.

For calculating the direct bandgap value  $(\alpha h\nu)^2$  versus  $h\nu$  is plotted and it is shown in the inset of Fig. 3. By extrapolating the straight portion of the graph on  $h\nu$  axis at  $\alpha = 0$ , the bandgap value is calculated as 4.02 eV, which is higher than that of bulk value of ZnS [2]. This blue shift of the bandgap takes place because of the quantum confinement effect.

Photoluminescence (PL) emission spectra from the ZnS:Ag sample as well as that of an undoped ZnS sample are measured at room temperature for an excitation wavelength of 250 nm and those are shown in Fig. 4. The Gaussian fittings of the measured PL spectrum from ZnS:Ag NPs is shown in the inset of Fig. 4. It can be seen that six emission

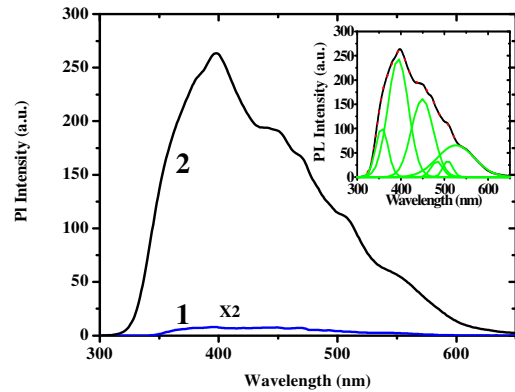


Figure 4: Photoluminescence (PL) emission spectra measured at room temperature after dispersing the samples in methanol. Curves marked as 1 and 2 correspond to undoped ZnS and silver doped ZnS, respectively. Inset shows the Gaussian fitting of the PL spectra of silver doped ZnS sample.

bands centered at 356.5, 393, 449, 483, 508, and 526 nm are present in the PL spectrum of ZnS:Ag sample. Out of the total six PL peaks, three peaks which are appeared at 393, 449, and 525 nm are most prominent ones and the intensity of 393 nm peak is the highest. The intensity of the emission band at 393 nm in ZnS:Ag sample is ~60 times more intense than that obtained in the undoped ZnS sample. It is seen that the measured PL emission bands appeared at energies below the band gap. This suggests that transitions from energy states lying above the band gap are not being favored for the luminescence process in the prepared ZnS:Ag NPs.

Previously, Eid *et. al* were reported such PL emissions from ZnS-phosphor doped with silver and cobalt [19]. Photoluminescence properties of ZnS NPs were reported that CTAB stabilized ZnS NPs in 350–450 nm region at 309 nm light excitation. In the presence of  $Ag^+$  ions the emission peak intensity up to 400 nm was reduced, while at 430 nm and 550 nm two new and stronger peaks appeared [18]. Similar results were obtained when Ag NPs solution was added to ZnS solution. The observations have been explained by the presence of interstitial sulfur and  $Zn^{2+}$ ,

especially near the surface of the nanocrystals and their interaction with various forms of silver. In addition, they reported diffusion of  $\text{Ag}^+$  ions into the lattice of the preformed ZnS NPs, just like the formation of  $\text{Ag}^+$  doped ZnS NPs and thus change the emission characteristics [18]. Manzoor *et al.* [20] were also reported PL emission from metallic ion doped ZnS NPs and the change in fluorescence peak observed were attributed to the effective radiative recombination of captured electron at the conduction band, or at the shallow trap energy level just below the conduction band with holes trapped at the energy level of  $\text{Ag}^+$  impurities above the valence band. Enhanced PL emission at 570 nm due to Ag impurity in Ag-doped CdZnS alloy quantum dots had also been reported very recently [21]. Considering that the energy of the emitted radiation in our ZnS:Ag sample at 393 nm is 3.16 eV and the position of the acceptor level introduced by silver in the energy gap at 0.85 eV [19] the bandgap of the sample comes out to be 4.01 eV, which matches well with the obtained value of 4.02 eV as the bandgap of ZnS:Ag nanoparticles from UV-visible absorption characteristics. The strongest PL peak appeared at 393 nm (~3.15 eV) in the ZnS:Ag NPs is due to the recombination of an excited electron either from the conduction band or some shallow traps just below the bottom of the conduction band with a positive hole captured at the acceptor level of silver. Photoluminescence emission appeared in the blue region peaked at 449 nm is attributed to defect-related emission of the ZnS host and the green peak appeared at 525 nm is due to a transition either from an impurity donor level or lattice defects at 0.91 eV below the lower edge of the conduction band to silver acceptor level.

#### 4. CONCLUSIONS

Here we have reported the synthesis of 0.5%  $\text{Ag}^+$  doped ZnS:Ag NPs capped with PVP via the chemical co-precipitation method. The formations of nanostructure of the samples have been confirmed by using XRD. The monodispersed size distribution of the synthesized ZnS:Ag NPs are confirmed from the analyses of HRTEM images and the average size of the synthesized NPs is 2.5 nm. A blue shift of the bandgap has been observed due to the quantum confinement effect. The Gaussian fittings of the measured room temperature PL spectrum from ZnS:Ag NPs shows the presence six emission bands centered at 356.5, 393, 449, 483, 508, and 526 nm. Out of the total six PL peaks, three peaks which are appeared at 393, 449, and 525 nm are most intense ones and the intensity of 393 nm peak is ~60 times higher than that obtained in the undoped ZnS sample. The appearance of the strongest band at 393 nm in ZnS:Ag sample is attributed to the recombination of an excited electron either from the conduction band or some shallow traps just below the bottom of the conduction band with a positive hole captured at the acceptor level of silver located at an energy 0.85 eV above the valence band. The blue peak appeared at 449 nm is attributed to defect-related emission of the ZnS host and the green peak appeared at 525 nm is attributed to a transition either from an impurity donor level

or lattice defects at 0.91 eV below the lower edge of the conduction band to silver acceptor level. The observation of enhanced PL emission in ZnS:Ag sample may be useful in designing future nanophotonic devices.

#### ACKNOWLEDGEMENTS

This work has been financially supported by DST Grant No. SR/FTP/PS-67/2008, Govt. of India. Authors are also grateful to TEQIP, Govt. of India for the partial financial support.

#### REFERENCES

- [1] R. N. Bhargava, D. Gallagher, X Hong, A. Nurmikko, *Phys. Rev. Lett.* 72, 416, 1994.
- [2] R. Sarkar, C. S. Tiwary, P. Kumbhakar, A. K. Mitra, *Physica E*, 40, 3115, 2008.
- [3] J. Yu, H. Lui, Y. Wang, W. Y. Jia, *J. Lumin.* 79, 19, 1998.
- [4] A. A. Khosravi, M. AngelKundu, L. Jatwa, S. K. Deshpande, *Appl. Phys. Lett.* 67, 2702, 1995.
- [5] P. Yang, M. K. Lu, D. Xu, D. Yuan, G. Zhou, *J. Phys. Chem. Solids*, 62 1181, 2001.
- [6] T. Ishihara, J. Takahasi, T. Goto, *Phys. Rev. B*, 42, 11099, 1990.
- [7] J. Hung, Y. Yang, S. Xue, B. Yang, S. Lui, J. Shen, *Appl. Phys. Lett.* 70, 2335, 1997.
- [8] J. Zhu, M. Zhou, J. Xu, X. Liao, *Mater. Lett.* 47, 25, 2001.
- [9] S.G. Counio, T. E. Gacoin, J.P. Boilot, *J. Phys. Chem.* 100, 2021, 1996.
- [10] M. Bruchez, M. Moronne, P. Gon, S. Weiss, A.P. Alivasatos, *Science*, 281 2013, 1998.
- [11] M. Chattopadhyay, P. Kumbhakar, C. S. Tiwary, R. Sarkar, A. K. Mitra, U. Chatterjee, *J. Appl. Phys.* 105, 024313, 2009.
- [12] M. Chattopadhyay, P. Kumbhakar, R. Sarkar, A. K. Mitra, *Appl. Phys. Lett.* 95, 163115, 2009.
- [13] R. Sarkar, P. Kumbhakar, A. K. Mitra, *Physics B*, 404 3855, 2009.
- [14] C. S. Tiwary, P. Kumbhakar, A. K. Mitra, K. Chattopadhyay, *J. Lumin.* 129, 1366, 2009.
- [15] A. A. Krasnov, J. P. Bender, W.Y. Kim, *Thin solid Films*, 467 247, 2004.
- [16] E. Hao, Y. Sun, B. Yang, X. Zhang, J. Liu, J. Shen, *J. Colloid and Interf. Sci.* 204 369, 1998.
- [17] A. Jungsik A. Billie, W. Brent, H. H. Paul, *J. Appl. Phys.* 95, 7873, 2004.
- [18] A. Murugadoss, A. Chattopadhyay, *Bull. Mater. Sci.* 31 533, 2008.
- [19] A. H. Eid, S. Mahmoud, S. N. Salama, *J. Mat. Sci.* 24 2860, 1989.
- [20] K. Manzoor, S. R. Vadera, N. Kumar, *Mater. Chem. Phys.* 82, 718, 2003.
- [21] R. Sethi, L. Kumar, P. K. Sharma, A. C. Pandey, *Nanoscale Res. Lett.* 5, 96, 2010.